Lamb Wave Based Non Destructive Evaluation of Weld Quality in Thin Section Friction Stir Joints

GOVINDA GAUTAM, MANISH KUMAR MEHTA, DHANASHRI M. JOGLEKAR and DHEERENDRA KR. DWIVEDI

ABSTRACT

Weld integrity assessment is critical for determining safety and dependability in the aerospace, civil, automotive, petrochemical as well as mechanical sectors. Non-Destructive Evaluation (NDE) based on Ultrasonic Guided Waves (UGW) is one of the finest emerging techniques for Structural Health Monitoring (SHM) systems, offering continual monitoring of similar, dissimilar, and composite materials. Traditional approaches need costly, time-consuming point-by-point examination, but Lamb wave based NDE has proven to be useful for wide-range, economical transmission, through-thickness, and in-situ inspection. The proposed study will conduct theoretical and experimental examinations of wave propagation through Al6061-Al5083 dissimilar Friction Stir Weld (FSW) of thin sections lap joints. In this investigation, two plates with thicknesses of 2mm each and dimensions of 250mm × 180mm are welded in a lap configuration with a fixed 30mm overlap length. Retro-reflective tape is attached at 30mm intervals on opposing sides of the stir zone. A Laser Doppler Vibrometer (LDV) is used to measure out-of-plane displacement of wave propagation. A high-voltage amplifier is utilized to generate 120V signals, along with that damping pastes are also used at sample boundaries to increase signal-to-noise ratios. Following NDE testing, weld samples were cross validated using SEM, Stereoscopy and CT scan enabling additional weld characterization.

Using a single variable (at a time) method, both fundamental modes i.e., antisymmetric (A0) and symmetric (S0) were employed for weld characterization through process parameter optimization, which included tool rotational speed (RPM), transverse speed (mm/min), and corresponding sound weld window. Frequency wavelength (f-k) filtering techniques have been utilized for mode separation and further signal processing. The operative signal is a modulated sinusoid with central burst at Gaussian packet signal of 60, 80 and 100kHz, respectively. A preliminary investigation reveals the frequency response dependence of rotational and transverse speed in signal transmission. When rotational speed increases and transverse speed decreases, signal transmission enhanced up to a point due to improved material mixing capability, i.e., weld quality, but then declines due to excessive heat input, resulting in weld discontinuities such as tunnel defects, wormholes, voids etc. Our experiment discovered a direct correlation between Lamb wave scattering and defect size, which dictates weld quality; as we surpass the welding window, the possibility of defects escalates. The S0 mode conversions produce abrupt transmission responses at 80kHz for 1300RPM rotation speed, 75mm/min transverse speed and corresponding joint W2.

Govinda Gautam[1], Manish Kumar Mehta[1], Dhanashri M. Joglekar[1], Dheerendra Kr. Dwivedi[1].

[1] Department of Mechanical and Industrial Engineering, Indian Institute of Technology Roorkee, 247667 Roorkee, Uttarakhand, India

INTRODUCTION

Friction stir welding (FSW) emerged as a new solid-state welding method [1], originating from TWI's invention in 1991 [2,3]. It has a large-scale application in industries such as aerospace, automotive, civil, marine, and petrochemical for its advantages, including dimensional stability, control of weld quality, environmental benefits etc. [4-6]. FSW has some constraints such as hole formation after welding, the essential large downward force requirement, and limitations on weld profiles. This welding process involves a non-consumable revolving tool that comprises both shoulder and pin that generates heat and facilitates material flow to produce the joint. The frictional heat generated by the tool's shoulder causes plastic deformation. The characteristics of the weld's microstructure are influenced by the tool's design, processing parameters, and rate of cooling. Much research has already been done focusing on optimized welding parameters and improved microstructure in FSW joints. Therefore, proper parameter selection is crucial to reduce defects and increase weld integrity [7].

Quality inspection of FSW welds is necessary to ensure performance during service. Traditional methods like visual inspection (VI), ultrasonic testing (UT), eddy-current testing (ECT), and acoustic emission (AE) have limitations in terms of labor, cost, and disruption to the structure. Guided waves (GWs), specifically Lamb waves, have been suggested as a continuous monitoring method for metallic and composite structures because of their ability to detect surface and internal cracks effectively. Various research studies have investigated the application of ultrasonic waves and GWs in the inspection of welds. These studies have focused on detecting, locating, and characterizing defects, as well as quantifying the size of cracks [8]. Numerous techniques in signal processing and pattern recognition have been employed to augment the process of damage detection. Recent research has focused on using Lamb waves to classify and assess defects in FSW plates. Linear correlations have been established between damage indices [9] and calculated damage volumes. This approach proves highly beneficial in evaluating elongated items such as pipes, rods, or rails due to its ability to propagate waves over extensive distances without notable amplitude attenuation. Numerous effective methodologies have also been devised to detect, pinpoint, and quantify structural impairments across several types of constructions [10-12].

Ultrasonic wave modes, including pulse-echo and pitch-catch, exhibit promising capabilities in the identification of flaws and concealed fractures within welded structures. Integrated laser-electromagnetic acoustic transducer (EMAT) systems have been used to evaluate fusion welds [13]. Additionally, studies have utilized Lamb waves in ultrasound immersion setups to assess the quality of FSW joints. This paper presented research findings regarding the propagation of Lamb waves in similar as well as dissimilar FSW joints without any defects. Friction stir welding experiments were conducted on metallic specimens, and data were captured using different sensing techniques. The captured signals were analyzed, and frequency-wavenumber filtering was employed to separate reflected waves from incident and transmitted waves. An ultrasonic Lamb wave-based method using an improved CEEMDAN approach [14] was developed for assessing the quality of FSW in magnesium alloy plates. The approach involved separating the fundamental mode, computing a damage index (DI) using amplitude fluctuations, and correlating the DIs with actual damage volumes determined

from CT images [15]. Overall, the research in this field aims to improve weld inspection techniques and ensure the quality and integrity of FSW joints.

Previous investigations have primarily concentrated on the transmission of guided waves (GWs) in a damped composite plate [16,17]. In these studies, the semi analytical finite element (SAFE) methods [18] were introduced, which integrated the Kelvin-Voigt damping model [19] to encompass the impact of anisotropic damping effects. Empirical outcomes acquired using a scanning Laser Doppler Vibrometer (LDV) exhibited satisfactory conformity with the anticipated waveforms [20]. Another analogous examination was conducted to explore circular damage in a square aluminum plate utilizing Lamb wave signals. For damage localization, a damage detection framework based on total focusing method through full matrix capture (TFM-FMC) was employed [21]. These techniques have been extensively employed in damage detection algorithms for an extended period. Their application involves the identification of fatigue cracking, delamination, and debonding in structural applications [22], utilizing the non-linear interaction of the fundamental anti-symmetric (A0) Lamb wave mode. Overall, GW-based non-destructive evaluation (NDE) methods present promising capabilities for the detection and assessment of damages in diverse structures, thereby contributing to the progression of non-destructive evaluation techniques.

Previous research has primarily focused on utilizing guided waves to monitor the health of structural joints, but there has been limited attention given to thin section solid-state welds. This research aims to bridge this gap by analyzing the Lamb waves propagation behavior for predicting the soundness of welds in thin section lap joints. The assessment of weld quality is conducted through both experimental and analytical investigations, utilizing three different frequency pulses. The study is divided into four main sections. The second section provides detailed information about the fabrication of welding joints using a CNC-based FSW setup with optimized process parameters. In the third section, dispersion behavior studies are conducted for both fundamental modes i.e., symmetric (S0) as well as antisymmetric (A0). Furthermore, this study showcases the application of the antisymmetric mode in non-destructive evaluation (NDE) across frequencies of 60kHz, 80kHz, and 100kHz. LDV testing and signal processing are employed in conjunction to evaluate the integrity of the welds. The fourth section offers a comprehensive explanation of the signal waveform used and detected after passing through the weld zone. To validate the effectiveness of the proposed inspection technique, various characterization techniques such as stereoscopy, CT scan, and SEM are utilized. Finally, in section five, the study concludes by summarizing the important findings and inferences derived from the research conducted.

FRICTION STIR WELDING

Al 6061-Al5083 thin section lap joint

Friction Stir Welding (FSW) employs a cylindrical tool with two primary parts, namely the shoulder and the pin, which undergo rotation. Positioned at the center of the overlapping sheets to be welded, the pin traverses along the designated path [23,24]. In general, pins should have a diameter of approximately 90% of the combined thickness of both plates. As the shoulder applies pressure against the plates and rotates, a strong

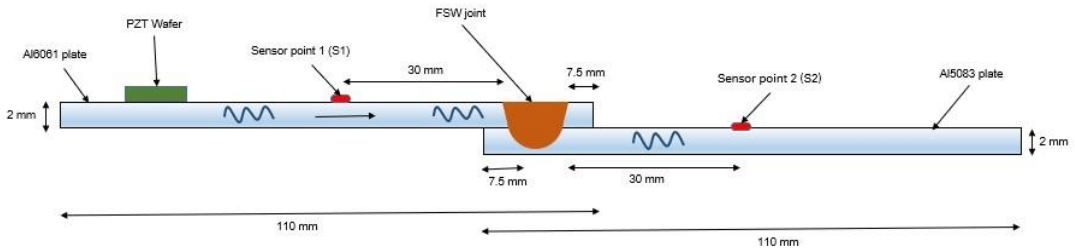

Figure 1: FSW Lap joint schematic of Al6061-Al5083

frictional force is generated [25]. This force, along with two major mechanisms namely frictional heating and plastic deformation [26], leads to the softening and mixing of the materials for joint formation.

In this study, lap joints were created by joining two dissimilar aluminum alloys, namely Al 6061 and Al 5083, each with a thickness of 2mm. A CNC based FSW machine was used to fabricate weld samples measuring 250mm by 180mm depicted above in figure 1. The average elastic properties of the materials used were as follows: density (d) = 2650kg/m3, Young's modulus (Y) = 71.2GPa, shear modulus (S) = 25.6GPa, and Poisson's ratio (μ) = 0.33. Used FSW setup, die steel tool, joint with defect (W4) and its SEM image are shown below in figure 2, 3(a) & (b) and 4, respectively.

During the welding process, the following FSW parameters were employed; the tool's rotational speed varied from 1200 to 1600rpm in increments of 100rpm, and the transverse speed ranged from 60 to 100mm/min with intervals of 10mm/min. These variations were made to fabricate samples with defects ranging from W1 to W5, while keeping all other process parameters constant. The fixed parameters for analyzing the effects of heat input on defect formation included a tool tilt angle of 2°, weld penetration depth of 3.67mm, overlap of 7.5mm, and the use of a die steel threaded tool with a 15mm shoulder diameter.

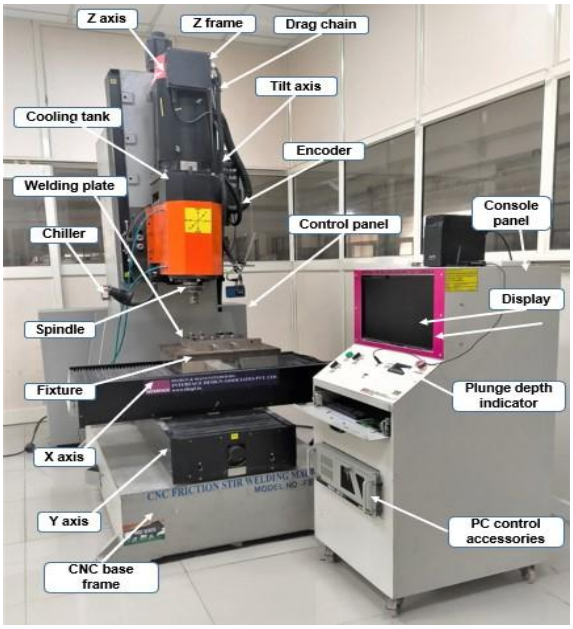

Figure 2: Friction Stir Welding setup

(a) (b)

Figure 3: (a) Die steel threaded FSW tool & (b) Joint with defect (W4)

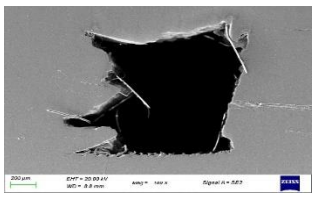

Figure 4: Friction Stir Welding setup

NON DESTRUCTIVE EVALUATION

Dispersion plot and A0 mode selection

This research focuses on investigating the transmission of the A0 mode of the Lamb wave. To overcome the challenges posed by the generation of multiple Lamb wave modes at higher frequencies [27,28], multiple lower frequencies of 60, 80 and 100kHz are utilized in this analysis. Additionally, the dominance of the A0 mode over the S0 mode and its higher out-of-plane displacement provides an advantageous feature for capturing the signal's data. To verify the transmission characteristics of the A0 mode in our research, we establish the nominal group velocity (C_g) using a combination of experimental measurements and numerical computations. An in-house semi-analytical finite element (SAFE) algorithm, implemented in MATLAB [29], is employed to generate the dispersion plot.

This algorithm considers the elastic properties of the weld samples under investigation and produces a dispersion curve for group and phase velocities, as illustrated in figure 5. The average group velocity estimated here is found to be 2848 m/s for the A0 mode. The experimentally determined group speed, which was obtained by evaluating the A-scan responses at two sensing points, can be calculated using

$$C_g = \frac{\Delta x}{\Delta t} \ , \ C_p = \frac{\omega}{k} \tag{1}$$

In this equation, Δx represents the distance between the two sensing locations on the sample and Δt is the peak time difference of the first wave packet of the acquired displacement versus time signal. Phase velocity (C_p) can also be estimated with the help of angular frequency (ω) and wavenumber (k). By applying equation (1),

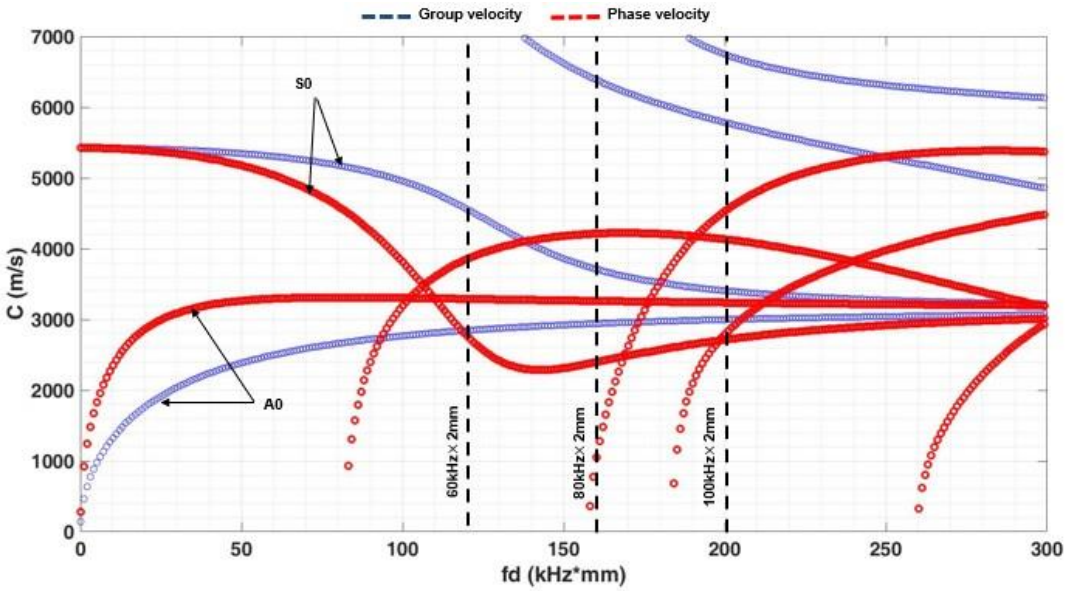

Figure 5: Dispersion curve for 2mm plate at various frequencies of 60, 80 and 100kHz

the experimental group velocity was determined to be 2796 m/s, which closely matches the numerically obtained group velocity. As a result, successful verification has been accomplished regarding the A0 mode of Lamb wave propagation.

Lamb wave actuation and sensing

To generate Lamb waves in the specimen, SP-5H piezo-electric transducers (PZTs) of the dimensions $25 \times 8 \times 1mm^3$ were used as actuators. Phenyl salicylate powder was employed to attach the PZTs onto the welded samples, securing them at 60mm before the stir zone. These piezoelectric wafers are renowned for their transducer qualities that couple strain, making them compact, lightweight, and inexpensive. When an electric current is applied, they can convert electrical energy into acoustic energy, resulting in the generation of Lamb waves through ultrasonic wave propagation within the structural material.

The experimental setup, as illustrated in figure 6, consisted of a single-point Laser Doppler Vibrometer (Polytec Inc.) equipped with a built-in function generator, a laser unit for scanning out-of-plane displacement, and a data acquisition system. A bipolar voltage amplifier was utilized to amplify the voltage signal generated by the function generator, increasing it from $6V_{pp}$ (peak-to-peak voltage) to $60V_{pp}$. To excite the Lamb wave signal, a longitudinal force was applied using a Hanning windowed tone burst with six cycles at frequencies of 60, 80, and 100 kHz. The input signal in both the time and frequency domain is depicted below in figure 7. The waves were generated from the location of the PZT and covered the entire lateral plane of the welded plate. Viscous damping tape was applied at the outer edge of the welded plate to prevent unwanted noise and signal reflections from the free edge boundary.

The Lamb wave signal was then detected at sensing points S1 and S2 using a laser head in a pitch-catch arrangement as it passed through the weld zone. S1 was positioned 30mm behind the lap weld zone, while S2 was located 30mm after the weld zone. These steps of actuation, sensing, and signal data acquisition were repeated for all five samples with defects of various sizes. Finally, the obtained displacement vs. time output data (signal) was further analyzed.

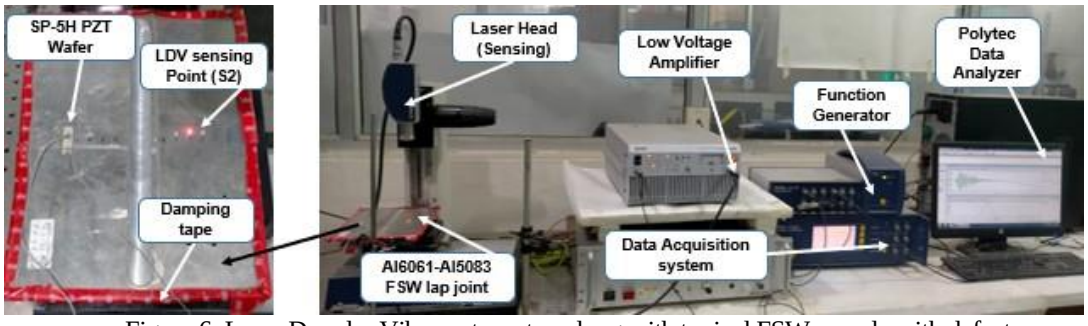

Figure 6: Laser Doppler Vibrometer setup along with typical FSW sample with defect

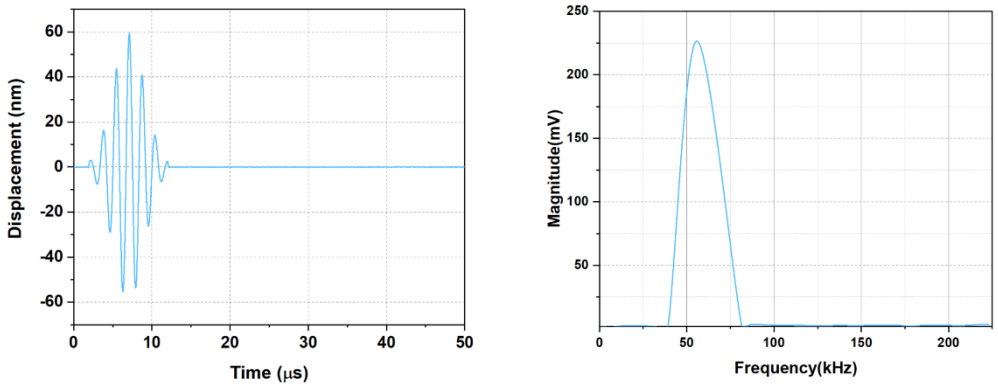

(a) (b)

Figure 7: Actuation signal waveform for 60kHz in (a) time and (b) frequency domain

RESULT AND ANALYSIS

The stir zone, which is the area of interest, is located between two sensing points, S1 and S2. These sensing points are positioned at an equal distance of 30mm from the stir zone. Lamb waves at frequencies of 60, 80, and 100KHz are used to examine thin section lap joints. Specifically, the low-frequency A0 mode is chosen due to its favorable low dispersion properties. To distinguish between different modes, a technique employing frequency-wavenumber filtering is utilized. The distances between the sensing points are carefully selected to effectively generate Lamb waves and ensure sufficient time separation between the modes. A0 to S0 mode conversion with corresponding time shift at 80kHz is depicted in figure 8(d). To enhance the analysis of the output signal, a Hanning window is applied to the low-frequency S0 mode signal, expediting the propagation from the time domain signal waveform. The equations governing the transmission loss and percentage of signal transmission have been employed for subsequent signal processing are as follows.

$$\text{Transmission loss (dB)} = 20 \log \frac{|FT[u1(t)]|}{|FT[u2(t)]|} \tag{2}$$

where, the actuation signal received at S1 is denoted as $u_1(t)$, while the sensing signal obtained after traversing a weld joint at S2 is represented as $u_2(t)$.

$$\% \text{ Signal transmission} = \frac{As}{Aa} \times 100 \tag{3}$$

where, S1 and S2 are the respective locations where peak amplitude values A_a and A_s are sensed respectively for the initial antisymmetric lobe. To identify the initial burst of propagating A0 wave mode, a Hanned time window was utilized on the reference signal. Actuating and sensing waveforms for W2 joint with defect are shown in figure 8. Excitation voltage of 120V and equal distance of 30mm are taken on opposite sides of the stir zone for all investigation.

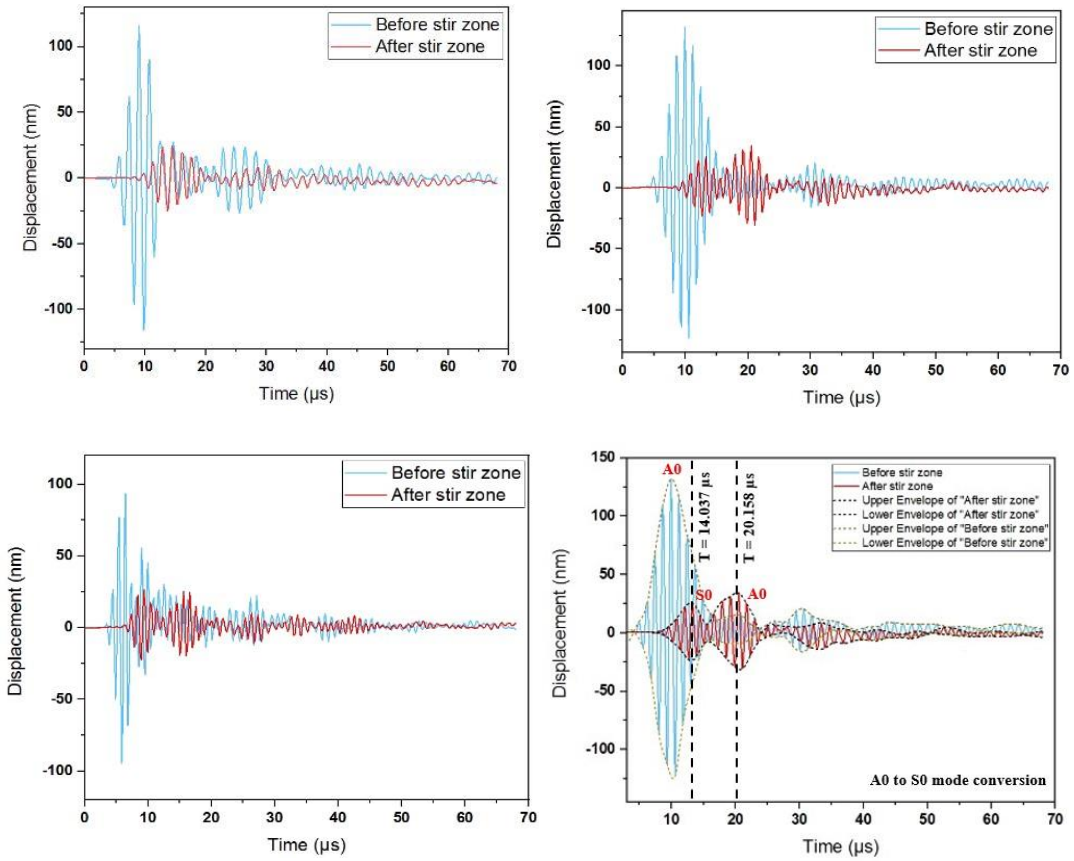

Figure 8: Recorded signal of actuator and sensor for W2 joint in time domain for the central excitation frequency of (a) 60kHz, (b) 80kHz, (c) 100kHz and (d) second envelope of captured waveform showing mode conversion.

Furthermore, Heat input index is utilized to establish the relationship between welding parameters i.e., rotational, and transverse speed with defect forming tendencies.

$$\text{Heat input index} = \frac{\omega 2}{v} \tag{4}$$

TABLE I: FSW SAMPLES WITH DEFECT CHARACTERISTICS

Weld samples with defect	**RPM (Revol-ution per min)**	**Trans-verse speed (mm/ min)**	**Heat input index (w^2/v) $\times 10^4$**	**Average defect size (mm)**	**Defect area (cm^2) $\times 10^{-3}$**	**Defect peri-meter (mm)**	**Loss at 60kHz (dB)**	**Loss at 80kHz (dB)**	**Loss at 100kHz (dB)**
W1	1200	60	2.40	0.48	3.304	2.30	6.34	7.82	8.13
W2	1300	70	2.42	0.96	6.597	3.49	7.64	14.79	8.21
W3	1400	80	2.45	1.12	7.328	3.52	10.85	11.35	9.02
W4	1500	90	2.50	1.45	8.035	3.99	13.53	12.58	9.92
W5	1600	100	2.56	1.93	12.75	4.55	14.90	15.66	12.57

where, ω is rotational speed in RPM and v is transverse speed in mm/min. Weld characteristics of all samples with defects i.e., RPM, transverse speed, heat input index and defect specifications i.e., average size, area as well as perimeter with corresponding losses are listed above in table I.

The evaluation of transmission losses was performed on different samples with defects depicted below in figure 9 showing the direct correlation between the average defect size and subsequent signal loss in transmission. Defect sizes in five welded joints namely W1 to W5 are 0.48mm, 0.96mm, 1.12mm, 1.45mm and 1.93mm, respectively. As average defect sizes in joints increase, their % transmission loss also increases from 8.13dB to 12.57dB because of inferior metallurgical continuity across the stir zone in normal to wave transmission direction. In other words, the percentage signal transmission decreases from 39.21% to 23.52% for 100kHz excitation frequency. The results suggest that the best quality welds with the least transmission loss are achieved when the rotational speed is set at 1200RPM and the transverse speed is maintained at 60mm/min, while keeping all other welding parameters constant. When the rotational speed increases but the transverse speed decreases, there is an increase in plastic deformation and frictional heating tendencies up to a certain threshold due to sufficient material flow velocity within the stir zone. However, beyond this threshold, excessive heat generation hampers the material mixing process, resulting in inferior joint formation and the occurrence of weld defects such as cracks, tunnel defects, flashes, and wormholes. These changes in the characteristics of the stir zone can be effectively assessed by comparing the behavior of Lamb wave propagation in welded structures.

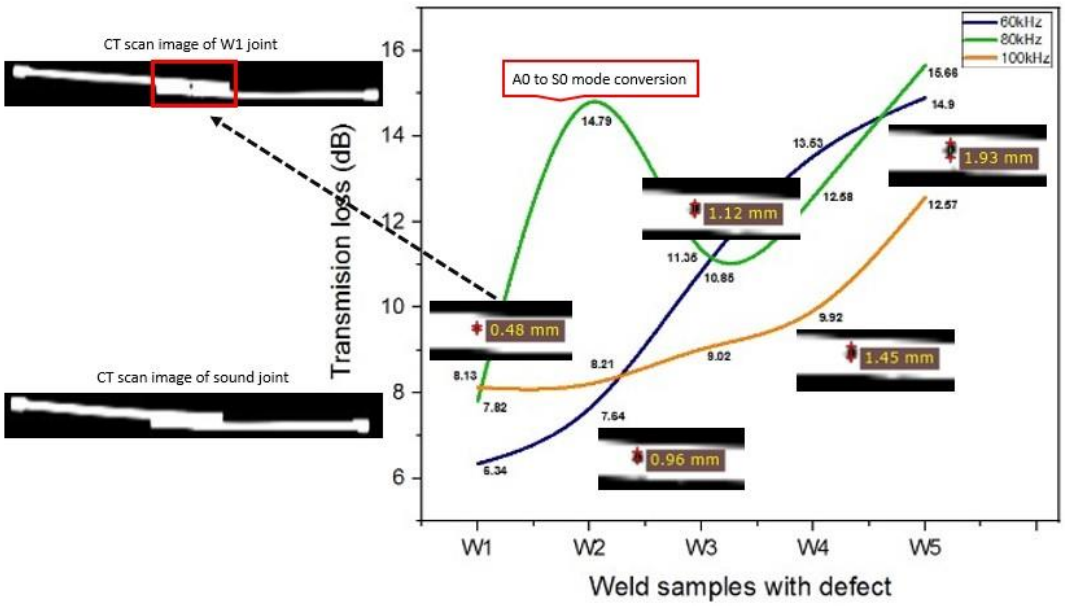

Figure 9: Transmission loss plot for five samples with defect (W1 to W5) and corresponding defect size from CT scan images

CONCLUSION

The present study aims to evaluate the weld quality in the thin section FSW joint by low frequency Lamb wave transmission. Weld integrity is predicted in terms of heat input index by estimating rotational and transverse speed process parameters. Excessive heat generated during welding can result in the formation of joints with defects, and these defects can be measured by analyzing wave characteristics such as transmission loss and percentage signal transmission. Several lap joints were evaluated, with varying defect sizes from 0.48mm to 1.93mm. The result of this investigation confirms the direct correlation between defect size and Lamb wave propagation behavior. To cross validate the findings, this investigation also incorporated various methods like SEM, CT scan, stereoscopy etc. As defect size increases, transmission loss increases from 8.13dB to 12.57dB for 100kHz and 120V. The abrupt changes in transmission loss observed in W2 can be attributed to a mode conversion from A0 to S0. The ability of this non-destructive technique to evaluate joint quality in thin sections suggests its potential for large-scale inspections of welded structures using Lamb wave.

REFERENCES

1. A.S. Babu, C. Devanathan, An overview of friction stir welding, *Int. J. Res. Mech. Eng. Technol.* 3 (2013) 259–265.
2. W. Thomas, E. Nicholas, J.C. Needham, M. Murch, P. Templesmith, C. Dawes, Friction stir welding, in: *International Patent Application no. PCT/ GB92102203 and Great Britain Patent Application*, 1991.
3. W. Thomas, M. Murch, E. Nicholas, P. Temple-Smith, J. Needham, C. Dawes, Improvements relating to friction welding, *Patent Number EP* 0653265,1995.
4. M. Muthukrishnan, K. Marimuthu, Some studies on mechanical properties of friction stir butt welded Al-6082-T6 plates, *Frontiers Automobile Mech.Eng.* (FAME) 2010 (2010) 269–273.
5. Y.-H. Zhao, S.-B. Lin, L. Wu, F.-X. Qu, The influence of pin geometry on bonding and mechanical properties in friction stir weld 2014 Al alloy, *Mater. Lett.* 59 (2005) 2948–2952.
6. N. Kumbhar, K. Bhanumurthy, Friction stir welding of Al 6061 alloy, *Asian J. Exp. Sci.* 22 (2008) 63–74.
7. H.A. Kumar, V.V. Ramana, An overview of friction stir welding (FSW): A new perspective, Research Inventy: *Int. J. Eng. Sci.* 4 (2014) 01–04.
8. W. Ostachowicz, P. Kudela, M. Krawczuk, A. Zak, I. Books24x, Guided Waves in Structures for SHM: The Time - domain Spectral Element Method vol. 1. *Hoboken: Wiley*, 2011
9. C.-T. Ng, M. Veidt, A lamb-wave-based technique for damage detection in composite laminates, *Smart Mater. Struct.* 18 (2009) 074006.
10. V.T. Rathod, D. Roy, Mahapatra, Ultrasonic Lamb wave based monitoring of corrosion type of damage in plate using a circular array of piezoelectric transducers, *NDT and E Int.* 44 (2011) 628–636.
11. A. Bagheri, K. Li, P. Rizzo, Reference-free damage detection by means of wavelet transform and empirical mode decomposition applied to Lamb waves, *J. Intelligent Mater. Syst. Struct.* 24 (2013) 194–208.
12. M.A. Fakih, S. Mustapha, M. Makki Alamdari, L. Ye, Symbolic dynamics time series analysis for assessment of barely visible indentation damage in composite sandwich structures based on guided waves, *J. Compos. Mater.* (2017), 0021998317696138.

13. Fakih, M. A., Mustapha, S., Tarraf, J., Ayoub, G., & Hamade, R. (2018). Detection and assessment of flaws in friction stir welded joints using ultrasonic guided waves: experimental and finite element analysis. *Mechanical Systems and Signal Processing*, 101, 516-534.
14. Garrett, Joseph Chandler, Hanfei Mei, and Victor Giurgiutiu (2022). An artificial intelligence approach to fatigue crack length estimation from acoustic emission waves in thin metallic plates. *Applied Sciences* 12.3, 1372.
15. Mahabunphachai, S., & Koç, M. (2010). Investigations on forming of aluminum 5052 and 6061 sheet alloys at warm temperatures. *Materials & Design* (1980-2015), 31(5), 2422-2434.
16. Gangwar, A. S., Y. Agrawal, and D. Joglekar. 2021. "Nonlinear interactions of Lamb waves with a delamination in composite laminates," *Journal of Nondestructive Evaluation, Diagnostics and Prognostics of Engineering Systems*, 4(3).
17. Radzie´nski, M., Ł. Doli´nski, M. Krawczuk, and M. Palacz. 2013. "Damage localisation in a stiffened plate structure using a propagating wave," *Mechanical Systems and Signal Processing*, 39(1-2):388–395.
18. Gangwar, A. G. and D. M. J. Joglekar. 2022. "Investigation of higher harmonic Lamb waves for facilitating delamination characterization," in *ECCOMAS Congress 2022-8th European Congress on Computational Methods in Applied Sciences and Engineering.*
19. Mei, H. and V. Giurgiutiu. 2019. "Guided wave excitation and propagation in damped composite plates," *Structural Health Monitoring*, 18(3):690–714.
20. Muller, A., B. Robertson-Welsh, P. Gaydecki, M. Gresil, and C. Soutis. 2017. "Structural health monitoring using Lamb wave reflections and total focusing method for image reconstruction," *Applied Composite Materials*, 24:553–573.
21. Gangwar, A. S., Y. Agrawal, and D. M. Joglekar. 2022. "Effects of Delamination on Higher Harmonics Generation in Unidirectional GFRP Laminate," in *Advances in Non Destructive Evaluation: Proceedings of NDE* 2020, Springer, pp. 411–421.
22. S. Burch, N. Bealing, A physical approach to the automated ultrasonic characterization of buried weld defects in ferritic steel, *NDT Int.* 19 (1986) 145
23. Singh, V. P., Patel, S. K., Ranjan, A., & Kuriachen, B. (2020). Recent research progress in solid state friction-stir welding of aluminum–magnesium alloys: a critical review. *Journal of Materials Research and Technology*, 9(3), 6217-6256.
24. Ma, Z. Y., Feng, A. H., Chen, D. L., & Shen, J. (2018). Recent advances in friction stir welding/processing of aluminum alloys: microstructural evolution and mechanical properties. *Critical Reviews in Solid State and Materials Sciences*, 43(4), 269-333.
25. Gite, R. A., Loharkar, P. K., & Shimpi, R. (2019). Friction stir welding parameters and application: A review. *Materials Today: Proceedings*, 19, 361-365.
26. Cai, W., Daehn, G., Vivek, A., Li, J., Khan, H., Mishra, R. S., & Komarasamy, M. (2019). A state-of-the-art review on solid-state metal joining. *Journal of Manufacturing Science and Engineering*, 141(3).
27. Sharma, Atul Kumar, et al. "Topology optimization of soft compressible phononic laminates for widening the mechanically tunable band gaps." *Composite Structures* 289 (2022): 115389.
28. Mitra, Aurovinda Kumar, Aparna A. Aradhye, and Dhanashri M. Joglekar. "Adiabatic Guided Wave Propagation through a Honeycomb Composite Sandwich Structure with Smoothly Varying Core Thickness." (2021)
29. Islam, M. M., and H. Huang. "Detecting severity of delamination in a lap joint using S-parameters." *Smart Materials and Structures* 27.3 (2018): 035006.